SEE COMMENTARY

Adolescent impatience decreases with increased frontostriatal connectivity

Wouter van den Bos[a,b,1], Christian A. Rodriguez[b], Julie B. Schweitzer[c,d], and Samuel M. McClure[b]

[a]Center for Adaptive Rationality, Max Planck Institute for Human Development, 14197 Berlin, Germany; [b]Department of Psychology, Stanford University, Stanford, CA 94305; [c]MIND Institute, University of California, Davis, School of Medicine, Sacramento, CA 95817; and [d]Department of Psychiatry and Behavioral Sciences, University of California, Davis, School of Medicine, Sacramento, CA 95817

Edited by Valerie F. Reyna, Cornell University, Ithaca, NY, and accepted by the Editorial Board May 4, 2015 (received for review December 3, 2014)

Adolescence is a developmental period associated with an increase in impulsivity. Impulsivity is a multidimensional construct, and in this study we focus on one of the underlying components: impatience. Impatience can result from (*i*) disregard of future outcomes and/or (*ii*) oversensitivity to immediate rewards, but it is not known which of these evaluative processes underlie developmental changes. To distinguish between these two causes, we investigated developmental changes in the structural and functional connectivity of different frontostriatal tracts. We report that adolescents were more impatient on an intertemporal choice task and reported less future orientation, but not more present hedonism, than young adults. Developmental increases in structural connectivity strength in the right dorsolateral prefrontal tract were related to increased negative functional coupling with the striatum and an age-related decrease in discount rates. Our results suggest that mainly increased control, and the integration of future-oriented thought, drives the reduction in impatience across adolescence.

adolescence | connectivity | impatience | delay discounting | DTI

Adolescence stands out as a particularly interesting developmental period because impulsivity seems to be greater at this age than during childhood or adulthood (1). This increased impulsivity is a part of healthy development and is thought to be crucial for the acquisition of skills needed for adult life (2, 3). However, increased impulsivity during adolescence also leads to unhealthy outcomes. For instance, compared with both children and adults, more teens need emergency department services secondary to accidents or experimenting with drugs or alcohol (4). Accidents are also the main reason for the increased mortality rate associated with adolescence (5). Certainly, an important contributor to the increase in negative outcomes is the increased access to risky situations (e.g., cars, alcohol, drugs, sexual activity) and decrease in parental oversight (6, 7). Nonetheless, impulsive behavior is elevated during this critical developmental period, highlighting the need to better understand the psychological and neural processes whose maturation across adolescence underlie these changes.

When investigating impulsivity it is important to recognize that it is a multidimensional construct. Impulsivity can be broken down into at least three independent components: acting without thinking, impatience, and sensation/novelty seeking (6, 8, 9). Importantly, each of these three components shows significant developmental trends across adolescence and each has been independently associated with self-reported risky behavior. For instance, research indicates that impatience is related to increased adolescent substance use and risk-taking (10–13). This study focuses on developmental changes in the construct of impatience.

Intertemporal choice paradigms have proven to be an effective tool for quantifying impatience. Numerous studies have shown that rates of delay discounting measured in these tasks decline with age and are correlated with adolescent academic success (14), substance use (15), conduct disorder (16), and a range of developmental disorders, including attention deficit hyperactivity disorder (ADHD) (17). Research suggests that multiple cognitive and neural processes underlie delay discounting (18–20). On the one hand, more impatient behavior can result from oversensitivity to immediate rewards (21). For example, there are several studies that show that people are more impatient when an immediate option is present compared with when both options are in the future (22). In addition, Luo et al. (23) showed that striatal activity is greater when participants are presented with immediate rewards versus preference-matched delayed rewards. On the other hand, more patient behavior may result from control processes that bias attention away from immediate rewards and/or emphasize the importance of future goals (24, 25). There are several studies that show that individual differences in future orientation are associated with more patient choices (1, 21, 26). Explicitly instructed future orientation leads to (*i*) within-subject reduction in discount rates (27–29) and (*ii*) increased activity in the brain's executive control network (30). Because there are (at least) two possible routes to greater or lesser impulsivity, it is challenging to determine how specific processes contribute to developmental differences by studying behavior alone. Here, we leverage our knowledge of the neural correlates of delay discounting to gain a deeper understanding of developmental changes in impatience.

Neuroimaging studies have consistently shown that delay discounting recruits corticostriatal circuitry (19). Generally, striatal circuits are divided into two networks: a ventral valuation network that is involved in representing the incentive value of the different options, and a dorsal control network that is involved in maintaining future goals and inhibiting prepotent responses (18, 24). Important nodes in the valuation network include regions

Significance

Compared with children and adults, teens and young adults often exhibit greater impulsivity and corresponding increases in emergency room visits, accidents from drug or alcohol use, and increased mortality risk. However, it remains poorly understood how increased impulsivity during adolescence may be explained in terms of brain and cognitive development. We focused on impatience, a central component of impulsiveness. We relate impatient behavior on a decision-making task to changes in connectivity within the brain's frontostriatal circuitry. Our results suggest that relative future orientation, not sensitivity to immediate rewards, determines adolescent impatience. These findings may help to design interventions to prevent the detrimental effects of adolescent impulsiveness and serve as a template for understanding neurodevelopmental disorders.

Author contributions: W.v.d.B., C.A.R., J.B.S., and S.M.M. designed research; W.v.d.B. and C.A.R. performed research; W.v.d.B. analyzed data; and W.v.d.B., C.A.R., J.B.S., and S.M.M. wrote the paper.

The authors declare no conflict of interest.

This article is a PNAS Direct Submission. V.F.R. is a guest editor invited by the Editorial Board.

See Commentary on page 8807.

[1]To whom correspondence should be addressed. Email: vandenbos@mpib-berlin.mpg.de.

This article contains supporting information online at www.pnas.org/lookup/suppl/doi:10.1073/pnas.1423095112/-/DCSupplemental.

associated with the mesolimbic dopamine system, particularly the ventral striatum, amygdala, and ventromedial prefrontal cortex. The control network includes the dorsal striatum, dorsal anterior cingulate cortex (dACC), dorsal and ventral lateral prefrontal cortex (dlPFC/vlPFC), and the posterior parietal cortex (19). Recent studies have shown that discount rates are not only associated with regional changes within the valuation and control networks, but also depend on the strength of connections within and between these networks (31). For instance, we recently showed that frontostriatal tracts predicted decreased delay discounting, whereas subcorticostriatal tracts predicted increased delay discounting in adults (21).

Neurodevelopmental models hypothesize that the different rates of maturation of the valuation and control networks account for increased impulsivity in adolescence. These models propose that there is a relatively early developing valuation system during adolescence, followed by a more slowly maturing cognitive control system (32, 33). Indications of the early development of the valuation system include increases in striatal dopamine levels, dopamine receptor availability, and blood oxygen level-dependent (BOLD) activity related to rewarding stimuli in early adolescence (34, 35) (but see refs. 36 and 37). In addition, many functional imaging studies, using tasks that require cognitive control, have shown increased engagement of lateral prefrontal areas across adolescence (38–40). These results raise the question of whether adolescents are impulsive because they are (*i*) more sensitive to immediate rewards, (*ii*) less capable of relying on the prefrontal cortex for self-control and future orientation, or (*iii*) both.

The current study was designed to investigate the processes underlying impatient behavior during the transition in and out of adolescence, and to determine how these behavioral changes relate to developmental changes in the structure and function of striatal circuits. We investigated developmental changes in behavior and brain in using a delay-discounting task. In addition, we used the Zimbardo Time Perspective Index (ZTPI) (41) to measure developmental changes in psychological components of impatient behavior—specifically, present hedonism (sensitivity to immediate rewards) and future orientation (control processes). Next, we used diffusion tensor imaging (DTI) to characterize different striatal tracts and their connectivity strength (42–45). Finally, we explored the structure–function relationship within structurally defined striatal tracts by performing psychophysiological interaction (PPI) analyses of functional magnetic resonance imaging (fMRI) data collected during the delay-discounting task (Fig. 1*A*). This multimodal developmental MRI study affords a unique perspective on normative development of impulsive behavior.

Results

Age, Temporal Discounting, and Future Orientation. To identify developmental trends across adolescence, we tested 50 participants (26 females) between the ages 8 and 25 y of age [mean (M) = 16.76; SD = 4.55]. Over this age range, maturation of brain systems may be (*i*) linear with respect to participants' ages; (*ii*) quadratic, with functioning peaking in midadolescence; or (*iii*) asymptotic, in the sense that changes occur between childhood and adolescence but stabilize in early adulthood (Fig. 1*B*). Robust linear regressions were used to take outliers into account when testing for each of these possible effects. Given that these developmental trends share variance, we did not use a single statistical model that included all three regressors. Instead, we performed independent linear regressions that incorporated one of the three age regressors and all independently significant age trends are reported (cf. ref. 46). In addition, we used Bayesian model comparison (Akaike information criterion and Bayesian information criterion) when analyses revealed multiple significant fits to provide some indication of the relative quality of the statistical models given the data.

Intertemporal preferences were assayed in two ways. First, we asked people to indicate their preferences between pairs of smaller, sooner (SS) and larger, later (LL) payments. Participants performed this task before and during fMRI scan acquisitions. The prescanner session was used to generate an estimate of each individual's discount rate (k), assuming a hyperbolic discount function, which was used to generate a subset of the decision problems for the scanner task. The experiment was incentive compatible; from both experiments, one choice was selected and paid after the experiment.

Given the high correlation between estimated discount rates between the prescanner and within-scanner tasks ($r = 0.84$, $P < 0.001$), we used the aggregate discount rate across both tasks (fitting all choices at the same time) as the individual difference measure of delay discounting. We used the log-transformed

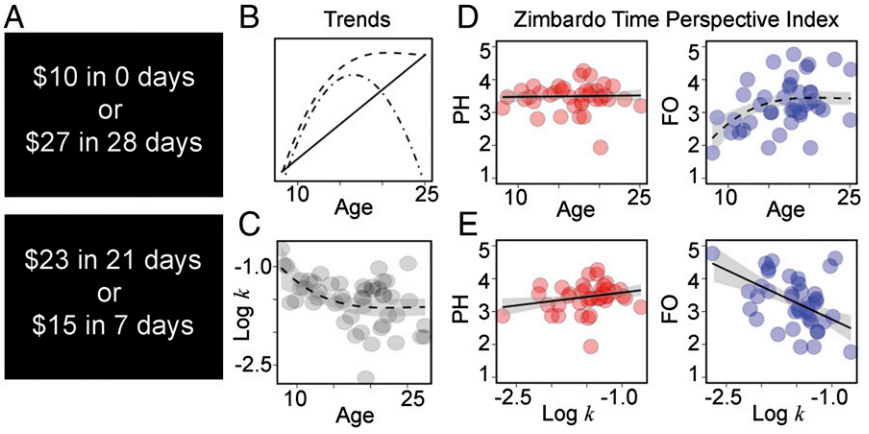

Fig. 1. (*A*) Participants made choices between smaller, sooner (SS) and larger, later rewards (LL) in the delay-discounting task. Participants were required to choose between both immediate and delayed rewards and between two delayed rewards. (*B*) Behavioral measures were analyzed for three potential dependencies on age: linear increase (mean centered), adolescent peak (i.e., linear increase^2), and adolescent emerging (i.e., adolescent peak × mean centered linear increase). (*C*) Discount rates estimated from the delay-discounting task were smaller with age across adolescence. (*D*) This change in delay discounting was reflected in an increase in future orientation but not present hedonism in the ZTPI. (*E*) Specifically, delay discount rates were not significantly correlated with measures of present hedonism, but were negatively correlated with self-reported future orientation. All age-related plots show the best-fitting age trend model in black, with shadowed error bars indicating SEM.

discount rates in all analyses because the distribution of estimated discount rates (k) was nonnormal (Shapiro–Wilk $W = 0.83$, $P < 0.001$). Discount rates varied by an order of magnitude across our study participants ($k_{min} = 0.002$ and $k_{max} = 0.19$). It is important to note that the quality of the hyperbolic model fits (i.e., best-fitting log-likelihood values) did not vary with age [all three (linear, peak, and emerging trends) values of $P > 0.38$)]. Additionally, there was no significant relationship between age and the estimated inverse temperature parameter (m; all three values of $P > 0.24$). The inverse temperature is a free parameter in the choice model that represents response noise. The choice function assumed that each individual will choose the option with the highest subjective value (which in many cases could be SS choice) with highest probability. Inconsistency in choices is captured by the inverse temperature parameter (see *Materials and Methods* for more details). That we did not find a relation between age and this parameter indicates that behavioral differences are not due to differences in choice variability. Also note that choice variability was not correlated with the discount rate k ($r = 0.11$, $P = 0.34$).

Our analyses revealed significant linear and asymptotic age effects in delay discount rates (k; linear: $r = 0.46$, $P < 0.001$; asymptotic: $r = 0.48$, $P < 0.001$; Fig. 1*C*). Thus, consistent with earlier studies (1, 47, 48), there was a decline in impatience across adolescence among our subjects. Bayesian model comparisons indicated that an asymptotic developmental trajectory with an accelerated decline in impulsive choices in early adolescence provided the best description of changes in discount rates with age (Table S1).

Finally, we tested for developmental changes in two subscales of the ZTPI relevant to our study: present hedonism and future orientation. In an earlier study (21), we found that present hedonism and future orientation independently predicted individual differences in discount rates of an adult population. For the current dataset, we found an increase in reported future orientation with age (linear: $r = 0.42$, $P < 0.005$; asymptotic: $r = 0.44$, $P < 0.004$; Fig. 1*D*). However, we did not find any age-related change in present hedonism (all three values of $P > 0.45$). Furthermore, we found that those participants who showed increased future orientation also made more patient choices in the intertemporal choice task ($r = -0.42$, $P < 0.005$; Fig. 1*E*). There was no relationship between present hedonism and discount rates ($r = 0.22$, $P = 0.17$; Fig. 1*E*). However, in line with our previous findings (21), we found that there was a significant relationship between individual differences in present hedonism and discounting when controlling for age ($r = 0.29$, $P < 0.05$).

Taken together, these results provide support for a cognitive control account of the development of temporal discounting. Control is believed to be specifically necessary for consideration of prospective future outcomes (29), and it is future orientation that appears to underlie age-related changes in impatience.

Imaging Analyses. Our next aim was to identify the relationship between frontostriatal circuitry and the developmental decrease in temporal discounting. We did this by way of a multistage, multimodal analysis. First, we determined the anatomical organization of the human striatum based on structural connectivity patterns. Next, based on an anatomical segmentation of the striatum, we mapped the developmental changes in the striatal tracts, and further specified tracts of interest (TOIs) using correlations between structural connectivity measures and delay discount rates. Finally, we hypothesized that the relationship between structural connectivity and impulsivity would be associated with changes in functional coupling. We therefore tested for changes in functional connectivity (PPIs) between the regions of interest (ROIs) that were associated with the TOIs in the structural analyses.

Structural Organization of Striatum Across Development. We began by determining the anatomical organization of the human striatum on the basis of the relative strength of white matter fiber connections from cortical and subcortical seed regions by applying a classification procedure to label each voxel in the striatum according to the target structure to which the voxel was most likely connected (42–45). To assess connectivity with extrastriatal regions, we used a set of 10 a priori target regions of interest (Fig. 2*A*). Consistent with the frontostriatal circuits previously identified in primates and other human diffusion MRI studies, this procedure resulted in individual segmentation maps with a ventromedial-to-dorsolateral gradient that was organized in bands of

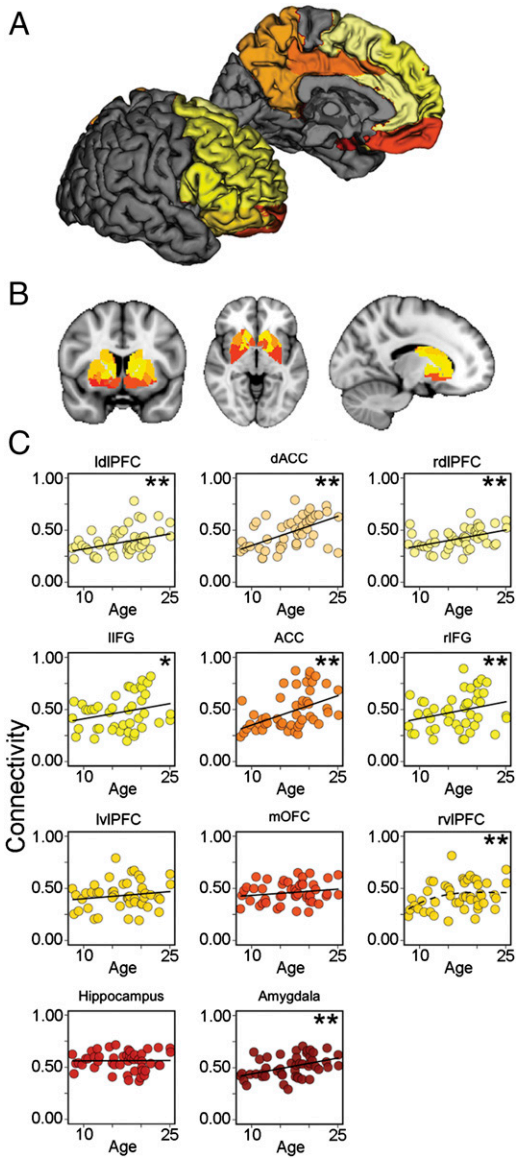

Fig. 2. (*A*) Target cortical and subcortical regions for striatal tractography were taken from the AAL atlas and are shown color-coded by region. (*B*) Individual striatal voxels were classified based on their most likely target. The results of this classification for one subject is shown with each voxel labeled according to the target region with which it was most strongly connected. (*C*) The likelihood of each corticostriatal tract was correlated with age across subjects. The results of these correlations are shown for each target ROI. Significant codes: $^{**}P < 4.545 \times 10^{-3}$ (i.e., Bonferonni-corrected threshold); $^{*}P < 10^{-2}$.

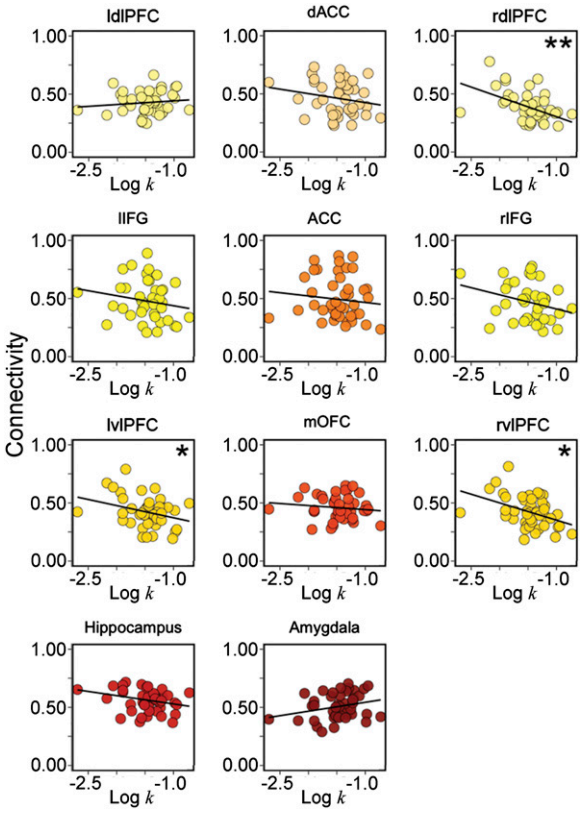

Fig. 3. Corticostriatal tract likelihoods were tested for correlation with delay discount rates (log *k*) separately for all ROIs. Tract strength between the striatum and different regions in lateral prefrontal cortex were negatively correlated with delay discount rates. Significant codes: $^{**}P < 4.545 \times 10^{-3}$ (i.e., Bonferonni-corrected threshold); $^{*}P < 10^{-2}$.

similar connectivity to subcortical and cortical regions (Fig. 2*B* and Fig. S1).

To arithmetically assess the intersubject spatial consistency of the striatal segments, we calculated the DICE coefficient, which measures the volume overlap of striatal subdivisions across subjects. The DICE values obtained for all striatal segments were high and satisfactory (between 0.32 and 0.59), except for the supplementary motor area (SMA) and posterior cingulate cortex (PCC) (DICE < 0.05; Table S2).

Structural Connectivity Analyses. To test whether developmental differences in discounting were related to the strength of white matter fiber tracts, we calculated the mean value of the tract probability within each striatal segment; we refer to this quantity as connectivity strength hereafter (cf. ref. 21). Data for the medial frontal target areas [medial orbitofrontal cortex (mOFC), ACC, and dACC], the hippocampus, and the amygdala, were averaged across hemispheres. Effects were considered significant at a Bonferroni-corrected α of 4.545×10^{-3} (i.e., $P = 0.05 \div 11$ tracts).

First, we tested for monotonic trends in the relationship between tract strength and age. We found that all tracts showed an increase in connectivity strength with age, except for the mOFC, the left vlPFC, and the hippocampus (Fig. 2*C* and Table S3). In addition, a linear age-related increase best described the data for all of the tracts except for the right vlPFC, which was best fit by the asymptotic trend.

We next aimed to determine which frontostriatal tracts were related to changes in delay discounting. First, we identified the tracts that were correlated with delay discount rates. Consistent with our previous findings (21), discount rates (log *k*) were negatively correlated with tract strength between medial striatum and the right dlPFC ($r = -0.47$, $P < 0.001$; Fig. 3 and Table 1). Stated a different way, participants with greater medial striatum–right dlPFC tract strength showed less impulsive behavior (smaller discount rates). Similar trends were found for the right ($r = -0.48$, $P = 0.007$) and left ($r = -0.37$, $P = 0.049$) vlPFC. It is notable that, in contrast with our previous results (21), we did not find that increased connectivity with the amygdala was associated with increased impulsiveness ($r = 0.26$, $P < 0.11$). However, the relationship between individual differences in amygdala tract strength and impulsivity may be masked by the overall developmental decrease in discounting and increase in striatum–amygdala tract strength. Indeed, amygdala tract strength was positively correlated with discount rates when controlling for age ($r = 0.65$, $P < 0.001$). Taken together, these results suggest that the development of the striatal connections with the lateral prefrontal cortex, particularly the right dlPFC, plays a role in age-related decrease in impulsivity.

Functional Analyses. For analysis of fMRI data during delay discounting, we first identified brain areas that were more greatly activated for choices when subjects chose LL rewards compared with when they chose SS rewards (while controlling for choice conflict). This contrast [i.e., LL – SS; familywise error (FWE) corrected, $P < 0.05$] identified regions in the right dlPFC [Montreal Neurological Institute (MNI) coordinates: 18, 26, 52], right vlPFC (MNI: 34, 38, −4), right parietal cortex (MNI: 30, −66, 44), and left cerebellum (MNI: −44, −64, −42). Each of these areas was more active when participants made LL compared with SS choices (Fig. 4*A*). We did not find any significant responses for the opposite (SS – LL) contrast.

We next tested whether choice-related differences in brain activity varied with age among our subjects. As with the anatomical connectivity analyses, we used three age trend regressors to test for possible age dependence. The linear decreasing and the asymptotic trend yielded highly overlapping whole-brain statistical maps, and showed age-related changes in right medial striatum (MNI: 12, 2, 8), left medial striatum (MNI: −13, 17, 8), and left temporoparietal junction (MNI: −55, −42, 23; Fig. 4*B*). Although these age trends in local activation follow a similar pattern to the age-related decline in discounting, these measures were not correlated across subjects ($r = 0.18$, $P = 0.16$). Together, these results are consistent with a recent large-scale study on adolescent discounting (49), which showed that, although the adolescents valued the same objective monetary rewards more than adults, this did not explain their increased impatient behavior on the intertemporal choice task.

Interestingly, the right medial striatum region overlapped with the striatal segment that we identified in the structural analyses to be connected with the dlPFC. To further quantify the age-related trends in this striatal region, we performed a post hoc

Table 1. Correlation between tract strength and discounting

	DLPFC	VLPFC	IFG
Laterality	*r*	*r*	*r*
Left	0.10	−0.48**	−0.13
Right	−0.47***	−0.37*	−0.18
	ACC	dACC	mOFC
	r	*r*	*r*
Medial	−0.11	−0.19	−0.04
	Amygdala	Hippocampus	
	r	*r*	
Bilateral	0.26	0.00	

*$P < .05$, **$P < .01$, ***$P < .001$.

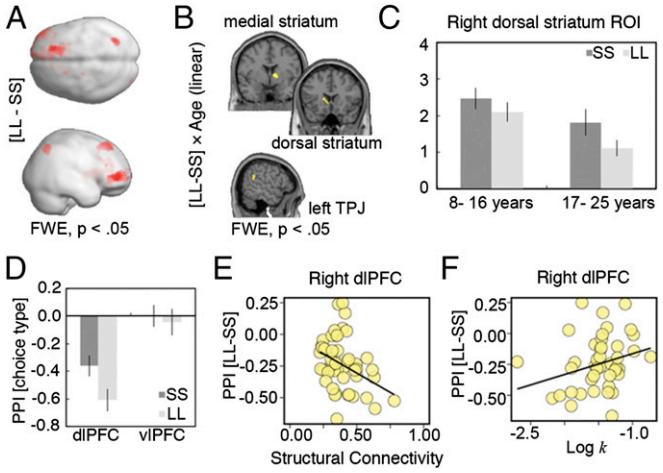

Fig. 4. (*A*) A whole-brain analysis of fMRI data was conducted to identify regions that were more activated when participants selected larger, later (LL) relative to smaller, sooner (SS) rewards (threshold at $P < 0.05$, FWE corrected). (*B*) A separate analysis was conducted to identify brain regions where activity depended on choice outcome (LL–SS) while accounting for possible age dependencies in responses (threshold at $P < 0.05$, FWE corrected). (*C*) Responses in the anterior medial striatum show that choice-related differences in brain activity were evident in older but not younger participants. (*D*) This age dependence in responses was reflected in functional connectivity between right dlPFC, right vlPFC, and their corresponding striatal segments. For each region, we plotted the change in functional connectivity for each choice type compared with baseline. (*E*) The negative functional connectivity between dlPFC and striatum was correlated with DTI-derived structural connectivity. (*F*) The changed in choice-related function connectivity was further related to estimated delay discount rates (log *k*).

ANOVA ROI analysis, which indicated that there was an overall reduction of striatal activity with age ($F = 6.26$, $P < 0.015$). More specifically, this age-related reduction was mainly driven by decreased medial striatal activity when subjects chose LL rewards ($F = 7.13$, $P < 0.009$; Fig. 4*C*), not SS rewards ($F = 2.13$, $P = 0.14$).

To investigate functional coupling of the prefrontal regions with the striatum, we used the functionally determined cortical ROIs together with the corresponding striatal segments derived from the structural analyses. These analyses revealed that the right dlPFC, but not the right vlPFC, showed a significant change in connectivity with the medial striatum during the decision period versus baseline [$t_{(47)} = -7.321$, $P < 0.001$, and $t_{(47)} = -0.92$, $P = 0.83$, respectively]. That is, there was increased negative coupling between the right dlPFC and the medial striatum during the decision phase of the delay-discounting task. More importantly, the negative coupling between the right dlPFC and the medial striatum was greater for choices of LL versus SS rewards [$t_{(47)} = 6.63$, $P < 0.001$; Fig. 4*D*]. This suggests that the increased right dlPFC activity during LL choices is associated with reduced medial striatal activity, which is consistent with the ROI analyses.

Finally, the difference in dlPFC–striatal functional connectivity between LL and SS trials correlated with structural connectivity ($r = 0.42$, $P < 0.004$; Fig. 4*E*), and discount rates ($r = 0.41$, $P < 0.005$; Fig. 4*F*). Taken together, these findings suggest that (*i*) the more patient participants showed increased negative coupling between right dlPFC and the medial striatum when choosing LL compared with when choosing SS rewards, and (*ii*) these participants also had stronger structural connectivity between the right dlPFC and the medial striatum.

Structural and Functional Development and Discounting. One interpretation of the current set of results is that the striatal tracts develop with age, leading to changes in structural and functional connectivity of the frontostriatal networks involved in inter-temporal decision making. Specifically, increased structural connectivity may allow for increased negative coupling between the right dlPFC and the medial striatum, which in turn may facilitate choices of LL over SS rewards. As such, the development of the dlPFC tract may contribute to the decrease in impulsive behavior that emerges across adolescence.

We explored this hypothesis more formally using a conditional processes analysis. We generated a serial mediator model that tries to capture the relation between age and discounting with two sequential mediators: structural and functional connectivity with the right dlPFC (Fig. 5). To test this mediation hypothesis, we used an ordinary least-square path analysis as implemented in Hayes' PROCESS algorithm (50). The 95% confidence interval around the indirect path was entirely above zero (0.05, 0.22). As such, the mediation analysis supports the hypotheses that an increase in dlPFC–medial striatum tract integrity with age leads to increased negative functional coupling between dlPFC and the medial striatum during LL versus SS choices, which finally leads to less impulsive decision making.

Specificity Analyses. Finally, we performed several analyses to determine whether our results were selective with respect to another critical impulse control measure: response inhibition as assayed using the stop signal reaction time (SSRT) (50). It is known that there are improvements in SSRTs across adolescence (51, 52), but also that behavior on this task is dependent on distinct neural pathways [i.e., inferior frontal gyrus (IFG)] from those involved in delay discounting. Consistent with previous findings, we found that SSRT decreased with age (linear: $r = 0.55$, $P < 0.001$; asymptotic: $r = 0.58$, $P < 0.001$; Fig. S2). However, there was no significant relation between SSRT and delay discounting in our data ($\log k$, $r = 0.25$, $P = 0.23$). Consistent with several studies (53), there was a significant correlation between SSRT and right IFG–striatum tract strength ($r = -0.31$, $P = 0.045$) but, importantly, not with structural and functional connectivity of the right dlPFC–striatum ($r = -0.15$, $P = 0.33$, and $r = 0.06$, $P = 0.66$, respectively; Fig. S2). In sum, these analyses suggest that the structural development of the right dlPFC striatal tract is specifically related to the processes involved in delay discounting (impatience) but not motor inhibition.

Discussion

Adolescence is a period strongly associated with impulsive behavior. Neurodevelopmental models (32, 33) have suggested that this may result from distinct developmental processes within the frontostriatal network, including (*i*) early maturation of the limbic system associated with increased appetitive behavior and preference for proximate rewards (34), and (*ii*) protracted development of the frontal cortex and frontostriatal connections, which are associated with the ability to regulate and control behavior (54). Similarly, neurocognitive models of delay discounting have posited a central role for separate components of

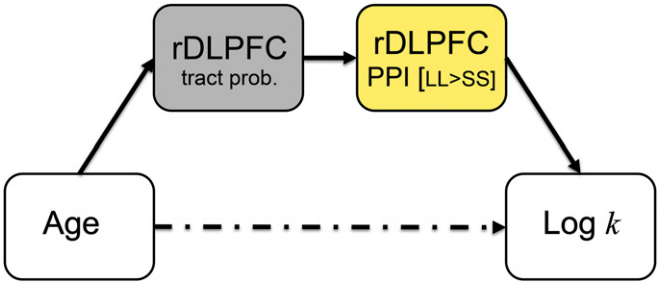

Fig. 5. Process model linking age related differences in brain structure, function, and behavior.

the frontostriatal network (18, 19, 21). The goal of the present study was to elucidate the role of specific processes related to developmental decreases in impatience.

There are three main contributions stemming from the results of this study. (*i*) Our behavioral and imaging results suggest that it is mainly increased control, not sensitivity to immediate rewards, that drives developmental reductions in impatience. (*ii*) This developmental decrease is related to increased future orientation and is accompanied by specific changes in functional and anatomical connectivity in medial striatal tracts connecting with dlPFC. (*iii*) Finally, because of our multimodal approach, we are able to integrate (up until now) isolated findings from functional and structural developmental neuroimaging studies.

In line with previous studies, we observed a decrease in discounting across adolescence. The nonlinear developmental trend suggests that impatient behavior peaks in early adolescence (1). Furthermore, we found that future orientation increased with age and was correlated with developmental decreases in discounting. However, we found no developmental differences in present hedonism or the immediacy effect. These latter measures also did not predict developmental differences in discounting. Taken together, these findings suggest a fundamental role for goal-oriented cognitive control processes in the developmental reduction in impatience, at least as assessed with intertemporal decision making. This interpretation is jointly supported by structural and functional imaging data.

In agreement with previous literature, we found that age was associated with an increase in structural connectivity strength in most of the identified striatal tracts (55). More interestingly, consistent with our previous results, increased strength of the medial striatum–dlPFC tract was selectively associated with a decrease in impatient behavior. In the context of development, changes in tract strength are believed to derive from myelination of prefrontal fibers, as histological measures demonstrate that this process extends into late adolescence (56). However, several structural properties may also contribute to tract likelihood, including myelination, axon caliber, axonal density, and membrane permeability (57). Regardless, given that most of these properties positively influence the flow of neuronal information (58), it can be assumed that developmental changes in structural connectivity provide information about the functional effectiveness of axonal connections.

Consistent with this interpretation, our results showed that developmental differences in structural connectivity are associated with changes in functional connectivity. That is, structural connectivity was related to increased negative functional coupling between the right dlPFC and the striatum when choosing LL versus SS rewards. These results support the hypothesis that increased efficiency in the inhibitory interaction between dlPFC and striatum is important for the development of intertemporal decision making. Of course, both probabilistic tractography and PPI are in principle unable to resolve the direction of connectivity. However, based on animal tracing studies, it is likely that the tracts between the striatum and prefrontal regions are afferent (i.e., providing input to the striatum) (58), suggesting the hypothesis that the reduction in impatience is due to top-down control. However, this hypothesis needs further testing, for instance, by using dynamic causal modeling to infer directionality (59).

Our results are consistent with the study by Christakou et al. (60) that found developmental increases in dlPFC engagement in an intertemporal choice task with hypothetical outcomes, and Olson et al. (61), who reported that developmental changes in prefrontal local (voxel-level) fractional anisotropy and mean diffusivity were related to developmental changes in discount rates. We extend these findings in two important ways: (*i*) we are able to specify the white matter tract involved; and (*ii*) we provide an integrative mechanistic account that relates developmental changes in structure to changes in function and finally behavior. That is, our data suggest that there is an increase in white matter connectivity strength with age, which in turn allows for increased efficiency in the inhibitory interaction between right dlPFC and striatum, potentially underlying the observed reduction of impatience with age.

Our findings suggest several future directions for study. First, it is noteworthy that we did not find any support for the hypothesis that sensitivity to immediate rewards drives adolescents' impatience. It is possible that absence of this effect is due to the low level of affective content of the stimuli used in the study. For instance, an earlier study on motor inhibition showed that there is an adolescent dip in impulse control in an emotional go–no-go task (using emotional faces as stimuli), but not in the nonemotional version of the task (62). In addition, they showed that the presence of emotional stimuli was accompanied by an adolescent peak in striatal activity. It has also been hypothesized that social stimuli and social context are particularly salient to adolescents (63, 64). For instance, there is evidence that the presence of peers specifically increases rates of delay discounting in adolescent populations (65, 66). Based on these findings, we hypothesize that it will be more likely to find a pattern of reward sensitivity that peaks in early adolescence in the context of such a social manipulation—both in terms of striatal activity and an immediacy effect in temporal discount rates. Based on our earlier reported relation between present hedonism and the ventral striatum–subcortical connectivity in adults (21), we expect that such as a social context effect will be most likely related to activity and connectivity of more ventral striatal regions. Given that adolescent risk behavior is often acted out in presence of peers (67), the addition of social components in future research may contribute to the understanding of the real-world consequences of developmental changes in impulsivity.

Second, impulsivity is a multidimensional construct and intertemporal choice tasks have been argued to only tap into one of its dimensions—impatience (8, 9). Our current data speak to this issue to some extent. That is, our specificity analyses suggest that the right dlPFC tract is associated with goal-oriented valuation, whereas the IFG tract is involved in inhibiting prepotent responses (based on external cues). These results further bolster our confidence that we were able to triangulate a specific neurodevelopmental mechanism underlying reductions in impatience with age. However, a recent study Steinbeis et al. (68) showed that there was a correlation between discount rates and behavior on the stop signal task within a group of children (6–13 y). In line with the interactive specialization account of neurodevelopment (69), this suggests that there may be an age-related increase in the specificity of the different striatal tracts. Adding more tasks that tap into additional dimensions of impulsivity, and extending the age range, could further our understanding of which neural systems are involved in the development of impulsive behavior.

Finally, we would like to point out how these results may advance current theoretical models of adolescent decision making. First, these results highlight the advantage of a detailed understanding, and mapping of, striatal circuitry, as has recently been argued by Casey (32). Mapping the circuitry highlights the important role of not only regional differences but also differences in connectivity strength (see also ref. 54). In addition, our results also suggest that research would benefit from greater specificity about regional differences within the striatum, rather than the oft-used division in ventral (nucleus accumbens) versus dorsal striatum (the rest). Consistent with conclusions based on decades of animal work (70, 71), our results indicate that the striatum is organized in a ventromedial-to-dorsolateral gradient. The dorsolateral striatum predominantly connected to sensorimotor-related regions, the ventromedial part collects visceral-related afferents, and striatal areas lying between these extremes receive higher order "associational" information. This organizational structure allows for at least a tripartite functional

division and introduces a role for context-dependent modulation of the more basic inhibitory and affect-related processes. Incorporating developmental changes in context sensitivity can potentially enrich current models that are mainly focused on reward sensitivity and response inhibition (see also refs. 63 and 72). Furthermore, our emphasis on the role of the development increase in context integration is in line with some key elements of fuzzy trace theory (FTT) (73). Rather than increased inhibition, FTT stresses the role of changes in representation/reasoning modes (gist versus verbatim) underlying developmental changes in decision making. Particularly, it posits that gist-based decision making develops with age, incorporating acquired experiences over time. Furthermore, fuzzy trace theory posits that prefrontal cortex contributes to cognitive control through better appraisal of decision options (74). Interestingly, neuroimaging (single-photon emission computed tomography and fMRI) studies have indicated that the gist mode of representation is mainly associated with increased activation in the prefrontal areas (for overview, see ref. 75). Still, future research is needed to understand how our results are related to a developmental shifts in reliance on, and quality of, gist-based representations in intertemporal choice.

In conclusion, our study expands the understanding of developmental changes in impulsive behavior across adolescence. By combining measures of structural connectivity, functional connectivity, and behavior, we were able to integrate several isolated findings from developmental studies that reported either only functional or only structural changes. This multimodel approach provides important insights on how functional connectivity may mediate the relationship between developmental changes in brain structure and changes in impulsive behavior and can serve as a template for future studies of developmental psychopathology, such as ADHD.

Materials and Methods

Participants. We recruited 50 participants (26 females) between ages of 8 and 25 y (M = 16.76; SD = 4.55) from a paid participant pool maintained by the Stanford University Psychology Department. Participants were paid $20 for participating in the MRI experiment, plus earnings from the discounting task. The study was approved by the Stanford University Institutional Review Board, and all participants gave written, informed consent before completing the task.

Behavioral Measures and Self-Report.

Delay-discounting task. Participants completed a total of 130 intertemporal choices in and outside the scanner (Fig. 1*A*). The 60 trials outside the scanner were determined by a staircase procedure. For this, the SS reward was fixed to $10 received today. The delay period (*D*) for the LL reward was randomly chosen from a uniform distribution between 15 and 60 d in the future. The size of the LL reward was adjusted to converge toward the same subjective value as the SS outcome. After the participants completed 60 trials on this task, we fitted data with the hyperbolic discount function:

$$V = A/(1 + kD), \quad [1]$$

where *A* is the amount in dollars of the LL reward. The individual discount rates that resulted from this procedure were used to generate the choice set of the delay-discounting task that was presented to participants in the scanner.

The SS delays in the fMRI task included 0 (today) and 14 d, and the LL delays included 14, 28, and 42 d. The different delays were equally divided over a total of 70 trials, resulting in 35 trials in which the SS was today and 35 trials in which the SS option was in the future (14 d). The SS rewards were randomly selected from a uniform distribution between $10 and $75. Following earlier studies, we determined LL reward size by adding a fixed percentage to the SS amount (0.5%, 1%, 5%, 10%, 15%, 20%, 25%, 30%, 50%, or 75%) for 48 out of the 70 trials. Next, for 22 of the 70 choices, we set the reward size of the LL exactly at the individually estimated indifference point using the estimated discount rates. These LL choices were randomly distributed over the task. Importantly, these task construction procedures led to individual choice sets that did not differ in level of choice conflict for different age groups (see below). Furthermore, using this range of choices, we were sure to include choices that were clearly in favor of the SS and the LL option. At the end of the experiment, one trial was randomly chosen from the total of set of 130 choices and paid to the participant in the form of a postdated check (this could be either a now or future choice).

Model fitting and manipulation checks. For the prescanner adaptive task, the initial discount rate *k* was set to 0.02 and was increased or decreased when the participant chose the SS or LL option, respectively. For the first 20 rounds, the step size for changes in *k* was set to 0.01, and after that the step size decreased by 5% for each following step. After the participants completed 60 choices, we used the multivariate constrained minimization function (fmincon) of the optimization toolbox implemented in MATLAB for model fitting. To model trial-by-trial choices, we used a softmax function to compute the probability (P_{SS}) of choosing the SS option on trial *t* as a function of the difference in V_{SS} and V_{LL}:

$$P_{SS} = \exp(m\ V_{SS}) / \left[\exp(m\ V_{SS}) + \exp(m\ V_{LL})\right], \quad [2]$$

where *m* is the inverse temperature and estimates response noise. This function assumed that each individual will choose the option with the highest subjective value (which in many cases could be SS choice) with highest probability. Inconsistency in choices is captured by the *m* parameter. Adding the inverse temperature function as a covariate of no interest to our regression models did not change any of the reported results. Individual discount rates were determined as the value of *k* that maximized the likelihood of the observed choices. The same fitting procedure was used for the scanner task.

The level of conflict on a trial is determined by the probability of choosing the one of the two options. Maximum choice conflict occurs when choice probability (P_{SS}) is 50%, and any deviation from 50% produces less conflict. Trial-by-trial conflict was computed as follows:

$$C = P_{SS} \times (1 - P_{SS}), \quad [3]$$

where $C = 0.25$ is the maximal conflict.

To check whether choice sets of the scanner task were comparable for different age groups, we correlated the average level of experienced conflict. First, we calculated the average level of conflict for the total choice set for each individual. This yielded two important results. First, it shows that the level of choice conflict is moderate (M = 0.12) and that there were no age differences in experienced choice conflict ($r = 0.17$, $P = 0.22$). Both are important requirements for the interpretation of developmental trends in the functional imaging data. Even if choice conflict were constant but very high (as is the case for most adaptive discounting task that quickly zoom in to the indifference point), this may result in developmental results that are specifically related to the need for maintaining high levels of cognitive control. To take into account the effect of possible outliers, all regressions with the discount rate were robust [using the robustbase package in R (76)].

The stop-signal task. We performed several analyses to test whether the reported associations between age, structural and functional connectivity were selective with respect to other impulse control measures. In particular, we investigated individual differences in the SSRT (77). This measure of impulse control is known to show developmental increases across adolescence (78), and with impulse control disorders, such as ADHD (79, 80), pathological gambling (81), and substance dependence (82). Importantly, some investigators argue that there is common neurocognitive component that underlies SSRT, delay discounting, and other measures of impulse control (83–85). However, others claim that these related constructs rely on different neurocognitive components (9). Thus, to examine the specificity of the neurocognitive component related to the right dlPFC–medial striatum tract, we investigated its relation between SSRT as measured with the stop signal task.

The stop signal task is a simple shape judgment task that requires subjects to respond differently to a square (right button) and a circle (left button). The participants are asked to respond as quickly as they can when they see the stimulus on the screen. On 75% of the trials, only the visual stimulus is presented, but on the other 25% of the trials, the so-called stop trials, the visual stimulus is followed by an auditory stop signal, indicating that participants should withhold their response. This task allows for an estimate of the covert latency of the stop process—the SSRT. For this experiment, we have used the default values of the STOP-IT program, and also the in-built analyses program ANALYZE-IT (77).

Time perspective. Traditionally, developmental psychologists have argued that adolescent impulsiveness derives mainly from a lack of future orientation (1, 86, 87). To measure time perspective, we used the ZTPI (41) because it gives a measure of both future orientation and present hedonism.

Pubertal development, sex, and IQ. Finally, given that previous studies have shown that delay discounting is associated with individual differences in

intelligence (48), we had participants complete the Raven Standard Progressive Matrices (88) to acquire an estimate of their visual-spatial IQ. First, we established that there was no relationship between age and IQ ($r = 0.16$, $P = 0.72$). Second, we found that there were also no correlations between IQ and log k ($r = 23$, $P = 0.46$).

Finally, it has been hypothesized that adolescent changes in reward-related behavior are caused by the impact of pubertal changes [e.g., hormones (63, 89)]. We collected data on pubertal status on a subset of our participants, but these did not reveal any significant relations to task behavior or neural measures (see *SI Materials and Methods* for more details). These results are in line with a recent study by de Water et al. (49), showing that self-reported pubertal stages were not related to temporal discounting in a large adolescent sample.

MR Data Acquisition and Preprocessing.

MRI data. Before participants went into the scanner, they were extensively trained in an on-site mock scanner using the MoTrak (PST, Inc.) head motion tracking system in combination with the Flock of Birds technology. MR data were collected on a 3-T GE Discovery MR750 scanner located at Stanford Center for Cognitive and Neurobiological Imaging. High-resolution T1-weighted images were first acquired [0.47 × 0.47 × 0.9 mm; repetition time (TR), 8.67 ms; echo time (TE), 3.47 ms; flip angle, 12°].

Diffusion-weighted imaging data. Diffusion-weighted imaging (DWI) was performed at a resolution of 0.85 × 0.85 × 2 mm, with three repeats of the b0 (no diffusion weighting image) and two repeats of each of 30 gradient directions at b1000 (TR, 9 s; TE, 89 ms). The FMRIB Diffusion Toolbox (FDT) (www.fmrib.ox.ac.uk/fsl/fdt) was used to correct the DTI data for head movement and eddy currents, tensor model fitting, and generating fractional anisotropy (FA) maps. Data from the two acquisitions of each diffusion direction were averaged to improve the signal-to-noise ratio.

fMRI data. Whole-brain BOLD weighted echo-planar images (TR, 2000 ms; TE, 30 ms; flip angle, 77°; 44 total slices with 2-mm slice gap; 64 × 64 matrix) were then acquired ∼30° off the anterior commissure–posterior commissure plane to maximize signal in the ventral prefrontal cortex and ventral striatum. fMRI data were analyzed using SPM8 (www.fil.ion.ucl.ac.uk/spm/). The first five volumes were not analyzed to accommodate T1 equilibration. Given the known problems of motion for connectivity analyses (90), we used ArtRepair software to correct for excessive movement (91). We have used the default values of ArtRepair to detect motion (threshold for movement at 0.5 mm/TR), and a rejection threshold when total of motion volumes would be larger than 5% of the total recorded volumes. Images were realigned in ArtRepair to correct for movement, smoothed with a 4-mm FWHM Gaussian kernel and motion adjusted. Deviant volumes resulting from sharp movement or spikes in the global signal were then interpolated using the two adjacent scans. No more than eight (median, 0; mean, 1.1) of the volumes were interpolated within any subject. There was no correlation between age and number of interpolated volumes ($r = 0.02$, $P = 0.89$; Fig. S3) We then applied slice-timing correction to all images. Next, motion correction to the first functional scan was performed using a six-parameter rigid-body transformation. The motion-corrected images was coregistered to each individual's structural MRI using a 12-parameter affine transformation. Images were then resampled into 3 × 3 × 3-mm voxels and spatially normalized to the MNI template by applying a 12-parameter affine transformation. Images were finally smoothed with a 4-mm isotropic Gaussian kernel and adjusted for global signal variation using a voxel-level linear model of the global signal.

Structural Connectivity Analyses.

Tractography. All diffusion image preprocessing and analyses were conducted using a combination of FSL tools and NiPy code (nipy.sourceforge.net/nipype/). The output of the FSL eddy correction was used to check for excessive head motion. None of the participants had to be rejected (threshold for movement was 1 voxel/TR). Tractography was performed in the subjects' native anatomical space, and the results were output in MNI space by providing transformation parameters estimated via a two-step procedure. First, the FA image was registered to each subject's high-resolution T1-weighted image with 6 df and a mutual information cost function. Next, the T1-weighted image was registered to the 1 × 1 × 1-mm MNI template using a nonlinear warping algorithm. The transformation parameters obtained from these two steps were concatenated to yield the mapping from the DWI to MNI space. The FDT toolbox was used to perform probabilistic tractography with a partial volume model (42) allowing for up to two fiber directions in each voxel. Dual-fiber models account for crossing fibers and thus yield more reliable results compared with single-fiber models. Five thousand sample tracts were generated from each voxel in the seed mask (striatum). Visual inspection ensured that tractography maps were successful and acceptable for further analysis. Tractography was performed separately for the left and right striatum, and possible tracts were restricted to the hemisphere of origin using an exclusion mask of the contralateral hemisphere.

Seed-based classification. Five thousand sample tracts were generated from each voxel in the seed mask (striatum). The striatal seed masks were based on combined striatal volumes of the subcortical segmentation implemented in freesurfer (surfer.nmr.mgh.harvard.edu/). Visual inspection ensured that tractography maps were successful and acceptable for further analysis. Tractography was performed separately for the left and right striatum, and possible tracts were restricted to the hemisphere of origin using an exclusion mask of the contralateral hemisphere. Seed-based classification was done by first thresholding the images such that only voxels with at least 10 samples were kept (21, 45, 92). Following standard procedures, voxel values were converted into proportions, such that the value at each voxel becomes the number of tracts reaching the target mask for that voxel, divided by the number of tracts that reach any of the 10 a priori target masks based on single or a combination of the standard automated anatomical labeling (AAL) maps [AAL map numbers within parentheses (21, 45)]: mOFC (28, 6, 26), vlPFC (10, 16), IFG (triangular partIFG: 14), dlPFC (4, 8), PCC (68), ACC (32), dACC (34), hippocampus (38), amygdala (42), and SMA (20). The striatum mask was based on the combined striatal volumes produced by the freesurfer subcortical segmentation algorithm. These AAL numbers all correspond to the left hemisphere; subtract 1 for right hemisphere values. This analyses resulted in 10 value maps, one for each target region, per participant. Finally, the striatum was segmented by assigning each voxel to the region with which it had the highest connection probability (Fig. 2*B* and Fig. S1) using FSL utilities (42).

DICE coefficients. To arithmetically assess the intersubject spatial consistency of the striatal segments, we calculated the DICE coefficient, which measures the volume overlap of striatal subdivisions across subjects. The DICE coefficient was estimated across subjects as the average overlap between a subject's striatal segment with striatal segments from each other subjects to assess if the method and underlying connections were reproducible across subjects (individual subjects' scans were nonlinearly registered to the MNI template). The DICE coefficient was calculated as follows:

$$DICE = 2.\ \frac{|ROI_1 \cap ROI_2|}{|ROI_1| + |ROI_2|}.100\%, \qquad [4]$$

where ∩ is the intersection of the ROI volumes and ranges from 0 to 1. Thus, the DICE coefficient ranges from 0%, for ROIs with no overlap up to 100% for identical ROIs.

Tract strength. To test whether individual differences in delay discounting were related to the strength of white matter fiber tracts, we calculated the mean value of the tract probability within each individually determined striatal segment. The resulting tract strength measure was correlated across subjects with log(k) using Spearman's rank-order correlation (tract strength values are nonnormally distributed, so nonparametric correlations are most appropriate) with total intracranial volume and segment size as covariates (21).

Functional Analyses.

General Linear Model. The fMRI time series data were modeled by a series of events convolved with a canonical hemodynamic response function (HRF) with additional time and dispersion derivatives to account for potential developmental related differences in the HRF. We set up a general linear model with a regressor that was 1 for choices in which subjects indicated a preference for the LL reward and 0 when the SS reward was chosen, which was modeled as a fixed event of 6-s duration. We used individual model-based parameters estimates of discount rate (k) to generate trial-by-trial measures of (*i*) total subjective value of the chosen option (V_{choice}) and (*ii*) a conflict regressor based on the probability of choice ("decision conflict"). These two measures were entered as covariates of no interest. The model also included session constants and motion parameters as regressors of no interest. First, we determined the areas that were involved in choosing LL over SS (and vice versa, few-corrected $P < 0.05$).

ROI analyses. We used the Marsbar toolbox to extract the parameter estimates from first-level single-subject contrasts using the functionally determined striatal ROIs based on the LL–SS contrast. Next, we divided the group in two by a median split on age; next, we ran ANOVA with choice type as within-subjects factor and age group as between-subjects factor.

PPI analyses. To perform PPI analyses, we extracted the mean BOLD time series from the voxels within a 6-mm radius sphere surrounding the activation peaks that fell within the right dlPFC and right VLPFC mask that were used for segmentation. As before, these spheres were combined with individual gray

matter masks to ensure analyses did not include signals from nonbrain or white matter voxels. Variance associated with the six motion regressors was removed from the extracted time series. The time courses were then deconvolved based on the model for the canonical hemodynamic response to construct a time series of neural activity following the procedures outlined in ref. 93. Finally, we used the Marsbar toolbox to extract mean PPI coefficients from first-level single-subject contrasts using the striatal segments that corresponded with the target area used for the PPI analyses (rDLPFC and rVLPFC).

ACKNOWLEDGMENTS. This study was funded by Netherlands Organization for Scientific Research Rubicon Grant 446-11-012 (to W.v.d.B.) and National Institute of Mental Health Grant R01 091068 (to S.M.M., W.v.d.B., and J.B.S.).

1. Steinberg L, et al. (2009) Age differences in future orientation and delay discounting. *Child Dev* 80(1):28–44.
2. Spear LPP (2000) The adolescent brain and age-related behavioral manifestations. *Neurosci Biobehav Rev* 24(4):417–463.
3. Spear LP (2013) Adolescent neurodevelopment. *J Adolesc Health* 52(2, Suppl 2): S7–S13.
4. Steinberg L (2007) Risk taking in adolescence: New perspectives from brain and behavioral science. *Curr Dir Psychol Sci* 16(2):55–59.
5. Eaton DK, et al.; Centers for Disease Control and Prevention (CDC) (2012) Youth risk behavior surveillance—United States, 2011. *MMWR Surveill Summ* 61(4):1–162.
6. Romer D (2010) Adolescent risk taking, impulsivity, and brain development: Implications for prevention. *Dev Psychobiol* 52(3):263–276.
7. Defoe IN, Dubas JS, Figner B, van Aken MA (2015) A meta-analysis on age differences in risky decision making: Adolescents versus children and adults. *Psychol Bull* 141(1): 48–84.
8. Whelan R, et al.; IMAGEN Consortium (2012) Adolescent impulsivity phenotypes characterized by distinct brain networks. *Nat Neurosci* 15(6):920–925.
9. Robbins TW, Gillan CM, Smith DG, de Wit S, Ersche KD (2012) Neurocognitive endophenotypes of impulsivity and compulsivity: Towards dimensional psychiatry. *Trends Cogn Sci* 16(1):81–91.
10. Reynolds B, Fields S (2012) Delay discounting by adolescents experimenting with cigarette smoking. *Addiction* 107(2):417–424.
11. Reynolds B (2006) A review of delay-discounting research with humans: Relations to drug use and gambling. *Behav Pharmacol* 17(8):651–667.
12. Audrain-McGovern J, et al. (2009) Does delay discounting play an etiological role in smoking or is it a consequence of smoking? *Drug Alcohol Depend* 103(3):99–106.
13. Romer D, Duckworth AL, Sznitman S, Park S (2010) Can adolescents learn self-control? Delay of gratification in the development of control over risk taking. *Prev Sci* 11(3): 319–330.
14. Duckworth AL, Seligman ME (2005) Self-discipline outdoes IQ in predicting academic performance of adolescents. *Psychol Sci* 16(12):939–944.
15. Madden GJ, Petry NM, Badger GJ, Bickel WK (1997) Impulsive and self-control choices in opioid-dependent patients and non-drug-using control participants: Drug and monetary rewards. *Exp Clin Psychopharmacol* 5(3):256–262.
16. Barkley RA, Edwards G, Laneri M, Fletcher K, Metevia L (2001) Executive functioning, temporal discounting, and sense of time in adolescents with attention deficit hyperactivity disorder (ADHD) and oppositional defiant disorder (ODD). *J Abnorm Child Psychol* 29(6):541–556.
17. Scheres A, Tontsch C, Thoeny AL, Kaczkurkin A (2010) Temporal reward discounting in attention-deficit/hyperactivity disorder: The contribution of symptom domains, reward magnitude, and session length. *Biol Psychiatry* 67(7):641–648.
18. van den Bos W, McClure SM (2013) Towards a general model of temporal discounting. *J Exp Anal Behav* 99(1):58–73.
19. Peters J, Büchel C (2011) The neural mechanisms of inter-temporal decision-making: Understanding variability. *Trends Cogn Sci* 15(5):227–239.
20. Kalenscher T, Pennartz CMA (2008) Is a bird in the hand worth two in the future? The neuroeconomics of intertemporal decision-making. *Prog Neurobiol* 84(3):284–315.
21. van den Bos W, Rodriguez CA, Schweitzer JB, McClure SM (2014) Connectivity strength of dissociable striatal tracts predict individual differences in temporal discounting. *J Neurosci* 34(31):10298–10310.
22. Loewenstein GF, Prelec D (1992) Anomalies in intertemporal choice: Evidence and an interpretation. *Q J Econ* 107(2):573–597.
23. Luo S, Ainslie G, Giragosian L, Monterosso JR (2009) Behavioral and neural evidence of incentive bias for immediate rewards relative to preference-matched delayed rewards. *J Neurosci* 29(47):14820–14827.
24. Figner B, et al. (2010) Lateral prefrontal cortex and self-control in intertemporal choice. *Nat Neurosci* 13(5):538–539.
25. Hutcherson CA, Plassmann H, Gross JJ, Rangel A (2012) Cognitive regulation during decision making shifts behavioral control between ventromedial and dorsolateral prefrontal value systems. *J Neurosci* 32(39):13543–13554.
26. Daniel TO, Stanton CM, Epstein LH (2013) The future is now: Comparing the effect of episodic future thinking on impulsivity in lean and obese individuals. *Appetite* 71: 120–125.
27. Berns GS, Laibson DI, Loewenstein G (2007) Intertemporal choice—toward an integrative framework. *Trends Cogn Sci* 11(11):482–488.
28. Boyer P (2008) Evolutionary economics of mental time travel? *Trends Cogn Sci* 12(6): 219–224.
29. Peters J, Büchel C (2010) Episodic future thinking reduces reward delay discounting through an enhancement of prefrontal-mediotemporal interactions. *Neuron* 66(1): 138–148.
30. Benoit RG, Gilbert SJ, Burgess PW (2011) A neural mechanism mediating the impact of episodic prospection on farsighted decisions. *J Neurosci* 31(18):6771–6779.
31. Peper JS, et al. (2013) Delay discounting and frontostriatal fiber tracts: A combined DTI and MTR study on impulsive choices in healthy young adults. *Cereb Cortex* 23(7): 1695–1702.
32. Casey BJ (2015) Beyond simple models of self-control to circuit-based accounts of adolescent behavior. *Annu Rev Psychol* 66:295–319.
33. Ernst M (2014) The triadic model perspective for the study of adolescent motivated behavior. *Brain Cogn* 89:104–111.
34. Galván A (2013) The teenage brain: Sensitivity to rewards. *Curr Dir Psychol Sci* 22(2): 88–93.
35. Barkley-Levenson E, Galván A (2014) Neural representation of expected value in the adolescent brain. *Proc Natl Acad Sci USA* 111(4):1646–1651.
36. Lamm C, et al. (2014) Longitudinal study of striatal activation to reward and loss anticipation from mid-adolescence into late adolescence/early adulthood. *Brain Cogn* 89:51–60.
37. Bjork JM, Smith AR, Chen G, Hommer DW (2010) Adolescents, adults and rewards: Comparing motivational neurocircuitry recruitment using fMRI. *PLoS One* 5(7): e11440.
38. Bunge SA, Dudukovic NM, Thomason ME, Vaidya CJ, Gabrieli JDE (2002) Immature frontal lobe contributions to cognitive control in children: Evidence from fMRI. *Neuron* 33(2):301–311.
39. Ordaz SJ, Foran W, Velanova K, Luna B (2013) Longitudinal growth curves of brain function underlying inhibitory control through adolescence. *J Neurosci* 33(46): 18109–18124.
40. Crone EA (2009) Executive functions in adolescence: Inferences from brain and behavior. *Dev Sci* 12(6):825–830.
41. Zimbardo PG, Boyd JN (1999) Putting time in perspective: A valid, reliable individual-differences metric. *J Pers Soc Psychol* 77(6):1271–1288.
42. Behrens TEJ, et al. (2003) Non-invasive mapping of connections between human thalamus and cortex using diffusion imaging. *Nat Neurosci* 6(7):750–757.
43. Draganski B, et al. (2008) Evidence for segregated and integrative connectivity patterns in the human basal ganglia. *J Neurosci* 28(28):7143–7152.
44. Tziortzi AC, et al. (2014) Connectivity-based functional analysis of dopamine release in the striatum using diffusion-weighted MRI and positron emission tomography. *Cereb Cortex* 24(5):1165–1177.
45. Cohen MX, Schoene-Bake J-C, Elger CE, Weber B (2009) Connectivity-based segregation of the human striatum predicts personality characteristics. *Nat Neurosci* 12(1): 32–34.
46. Somerville LH, et al. (2013) The medial prefrontal cortex and the emergence of self-conscious emotion in adolescence. *Psychol Sci* 24(8):1554–1562.
47. Green L, Fry AF, Myerson J (1994) Discounting of delayed rewards. A life-span comparison. *Psychol Sci* 5(1):33–36.
48. Olson EA, Hooper CJ, Collins P, Luciana M (2007) Adolescents' performance on delay and probability discounting tasks: Contributions of age, intelligence, executive functioning, and self-reported externalizing behavior. *Pers Individ Dif* 43(7): 1886–1897.
49. de Water E, Cillessen AHN, Scheres A (2014) Distinct age-related differences in temporal discounting and risk taking in adolescents and young adults. *Child Dev* 85(5): 1881–1897.
50. Hayes A (2013) *Introduction to Mediation, Moderation, and Conditional Process Analysis: A Regression-Based Approach*. Methodology in the Social Sciences (The Guilford Press, New York).
51. Schel MA, Scheres A, Crone EA (2014) New perspectives on self-control development: Highlighting the role of intentional inhibition. *Neuropsychologia* 65:236–246.
52. Vink M, et al. (2014) Frontostriatal activity and connectivity increase during proactive inhibition across adolescence and early adulthood. *Hum Brain Mapp* 35(9):4415–4427.
53. Liston C, et al. (2006) Frontostriatal microstructure modulates efficient recruitment of cognitive control. *Cereb Cortex* 16(4):553–560.
54. Somerville LH, Casey BJ (2010) Developmental neurobiology of cognitive control and motivational systems. *Curr Opin Neurobiol* 20(2):236–241.
55. Giedd JN (2004) Structural magnetic resonance imaging of the adolescent brain. *Ann N Y Acad Sci* 1021:77–85.
56. Huttenlocher PR (1979) Synaptic density in human frontal cortex—developmental changes and effects of aging. *Brain Res* 163(2):195–205.
57. Jones DK, Knösche TR, Turner R (2013) White matter integrity, fiber count, and other fallacies: The do's and don'ts of diffusion MRI. *Neuroimage* 73(C):239–254.
58. Paus T (2010) Growth of white matter in the adolescent brain: Myelin or axon? *Brain Cogn* 72(1):26–35.
59. Friston KJ, Harrison L, Penny W (2003) Dynamic causal modelling. *Neuroimage* 19(4): 1273–1302.
60. Christakou A, Brammer M, Rubia K (2011) Maturation of limbic corticostriatal activation and connectivity associated with developmental changes in temporal discounting. *Neuroimage* 54(2):1344–1354.
61. Olson EA, et al. (2009) White matter integrity predicts delay discounting behavior in 9- to 23-year-olds: A diffusion tensor imaging study. *J Cogn Neurosci* 21(7):1406–1421.
62. Somerville LH, Hare T, Casey BJ (2011) Frontostriatal maturation predicts cognitive control failure to appetitive cues in adolescents. *J Cogn Neurosci* 23(9):2123–2134.
63. Crone EA, Dahl RE (2012) Understanding adolescence as a period of social-affective engagement and goal flexibility. *Nat Rev Neurosci* 13(9):636–650.

64. van den Bos W (2013) Neural mechanisms of social reorientation across adolescence. *J Neurosci* 33(34):13581–13582.
65. Brien LO, et al. (2011) Adolescents prefer more immediate rewards when in the presence of their peers. *J Res Adolesc* 21(4):747–753.
66. Weigard A, Chein J, Albert D, Smith A, Steinberg L (2014) Effects of anonymous peer observation on adolescents' preference for immediate rewards. *Dev Sci* 17(1):71–78.
67. Albert D, Chein J, Steinberg L (2013) Peer influences on adolescent decision making. *Curr Dir Psychol Sci* 22(2):114–120.
68. Steinbeis N, Haushofer J, Fehr E, Singer T (2014) Development of behavioral control and associated vmPFC-DLPFC connectivity explains children's increased resistance to temptation in intertemporal choice. *Cereb Cortex*, 10.1093/cercor/bhu167.
69. Johnson MH (2011) Interactive specialization: A domain-general framework for human functional brain development? *Dev Cogn Neurosci* 1(1):7–21.
70. Haber SN, Knutson B (2010) The reward circuit: Linking primate anatomy and human imaging. *Neuropsychopharmacology* 35(1):4–26.
71. Voorn P, Vanderschuren LJMJ, Groenewegen HJ, Robbins TW, Pennartz CMA (2004) Putting a spin on the dorsal-ventral divide of the striatum. *Trends Neurosci* 27(8): 468–474.
72. Pfeifer JH, Allen NB (2012) Arrested development? Reconsidering dual-systems models of brain function in adolescence and disorders. *Trends Cogn Sci* 16(6):322–329.
73. Reyna VF, Brainerd CJ (2011) Dual processes in decision making and developmental neuroscience: A fuzzy-trace model. *Dev Rev* 31(2-3):180–206.
74. Chick CF, Reyna VF (2012) A fuzzy-trace theory of adolescent risk-taking: Beyond self-control and sensation seeking. *The Adolescent Brain: Learning, Reasoning, and Decision Making*, eds Reyna VF, Chapman SB, Dougherty MR, Confrey J (American Psychological Association, Washington, DC), pp 379–428.
75. Chapman SB, Gamino JF, Mudar RA (2012) Higher order strategic gist reasoning in adolescence. *The Adolescent Brain: Learning, Reasoning, and Decision Making*, eds Reyna VF, Chapman SB, Dougherty MR, Confrey J (American Psychological Association, Washington, DC), pp 123–151.
76. Todorov V, Filzmoser P (2009) An object-oriented framework for robust multivariate analysis. *J Stat Softw* 32(3):1–47.
77. Verbruggen F, Logan GD, Stevens MA (2008) STOP-IT: Windows executable software for the stop-signal paradigm. *Behav Res Methods* 40(2):479–483.
78. Bedard A-C, et al. (2002) The development of selective inhibitory control across the life span. *Dev Neuropsychol* 21(1):93–111.
79. Crosbie J, et al. (2013) Response inhibition and ADHD traits: Correlates and heritability in a community sample. *J Abnorm Child Psychol* 41(3):497–507.
80. Soreni N, Crosbie J, Ickowicz A, Schachar R (2009) Stop signal and Conners' continuous performance tasks: Test–retest reliability of two inhibition measures in ADHD children. *J Atten Disord* 13(2):137–143.
81. Brevers D, et al. (2012) Impulsive action but not impulsive choice determines problem gambling severity. *PLoS One* 7(11):e50647.
82. de Wit H (2009) Impulsivity as a determinant and consequence of drug use: A review of underlying processes. *Addict Biol* 14(1):22–31.
83. Berkman ET, Burklund L, Lieberman MD (2009) Inhibitory spillover: Intentional motor inhibition produces incidental limbic inhibition via right inferior frontal cortex. *Neuroimage* 47(2):705–712.
84. Berkman ET, Graham AM, Fisher PA (2012) Training self-control: A domain-general translational neuroscience approach. *Child Dev Perspect* 6(4):374–384.
85. Tabibnia G, et al. (2011) Different forms of self-control share a neurocognitive substrate. *J Neurosci* 31(13):4805–4810.
86. Nurmi J (1991) How do adolescents see their future? A review of the development of future orientation and planning. *Dev Rev* 11(1):1–59.
87. Furby L, Beyth-Marom R (1992) Risk taking in adolescence: A decision-making perspective. *Dev Rev* 12(1):1–44.
88. Raven JC (1941) Standardization of progressive matrices. *Br J Med Psychol* 19(1): 137–150.
89. Peper JS, Dahl RE (2013) The teenage brain: Surging hormones—brain–behavior interactions during puberty. *Curr Dir Psychol Sci* 22(2):134–139.
90. Power JD, Barnes KA, Snyder AZ, Schlaggar BL, Petersen SE (2012) Spurious but systematic correlations in functional connectivity MRI networks arise from subject motion. *Neuroimage* 59(3):2142–2154.
91. Mazaika P, Hoeft F, Glover GH, Reiss AL (2009) Methods and Software for fMRI Analysis for Clinical Subjects. *Human Brain Mapping*. Available at cibsr.stanford.edu/tools/human-brain-project/artrepair-software.html. Accessed May 26, 2015.
92. Forstmann BU, et al. (2012) Cortico-subthalamic white matter tract strength predicts interindividual efficacy in stopping a motor response. *Neuroimage* 60(1):370–375.
93. Gitelman DR, Penny WD, Ashburner J, Friston KJ (2003) Modeling regional and psychophysiologic interactions in fMRI: the importance of hemodynamic deconvolution. *Neuroimage* 19(1):200–207.
94. Petersen AC, Crockett L, Richards M, Boxer A (1988) A self-report measure of pubertal status: Reliability, validity, and initial norms. *Journal of Youth and Adolescence* 17(2): 117–133.